CONF-861114--24

DE87 002408

"Angular Distributions of Very Low Energy Recoil Ions"

C.E.González Lepera, M.Breinig, J.Burgdörfer, R.DeSerio, S.B.Elston, J.P.Gibbons, H-P. Hülskötter[a], L.Liljeby[b], C.R.Vane and I.A.Sellin.

The University of Tennessee, Knoxville,TN 37916 and
Oak Ridge National Laboratory, Oak Ridge, TN 37831

Abstract

We present the first measurements of the angular distribution of recoil ions near 90° with respect to the incident projectile direction. Beams of 22.5 and 33 MeV chlorine ions (incident charge states q =4,5,8) have been used as "hammer" beams incident on Ne atoms.

We confirm the long standing assumption that these recoil ions are ejected preferentially at angles near 90° with respect to the primary beam direction and with energies typically less than 5 eV. Recoil ions ejected around 90° have an energy distribution appreciable wider than those ejected at either larger or smaller angles.

(a) Present Address: Physics Department, Stan ford University, Stanford, CA 94305, USA

(b) On visit from Institute of Microwave Technology, P.O.Box 70033 S/10044-Stockholm, Sweden

Introduction

A great deal of effort has been devoted in the past decade to the study of highly charged low energy recoil ions. K x-ray target spectroscopy[1] first suggested that a fast-moving highly stripped ion beam colliding with Ne atoms can produce hydrogenlike Ne ions in appreciable amounts. The results of Cocke[2] proved that recoil ions are produced with cross-sections high enough to make secondary recoil ion sources practical for a variety of low-energy experiments[3].

Two different models have been used[2] to predict the dependence of the production cross section on recoil ion charge state. The independent particle model (IPM) assumes that electron ejection from the target occurs sequentially and independently. The impact parameter dependent probability $P_n(b)$ for ejection of n electrons can then be found using binomial statistics. The IPM approach was taken by Olson[4] who used a classical-trajectory Monte Carlo (CTMC) calculation to obtain the single electron ejection probability $P(b)$. More recently, Horbatsch[5], using a quantum statistical semiclassical method to describe the time evolution of the target electron density, presented results which agree substantially better with experiments. On the other hand, the energy deposition model, developed by Russek and collaborators[6], proposes a two step process. First, during the collision, part of the translational energy of the system is transferred as electronic excitation to projectile and target. In a second step after the collision, this excitation energy is shared between electrons, allowing autoionization to define the final charge state. Cocke[2] compared his experimental results with the predictions of both models and found that the CTMC is more appropriate to describe the lower ionization states of the target while the energy deposition model accounted for most of the features of the higher recoil ion charge states.

To the best of our knowledge all experimental information

concerning production mechanisms of low energy recoil ions is available in the form of total cross sections, including the results of coincidence experiments between projectile and recoil charge states by Gray[7] et al., but no data are available on differential cross sections for recoil ion production.

Experimental Method

Chlorine beams of variable energy and charge state were provided by the Oak Ridge National Laboratory EN Tandem Van de Graaff accelerator. The primary ion beam was charge state selected and collimated by a 1.5 mm circular aperture. The projectiles were incident on a Ne target located at the rotation center of the detection system. Fig.1 shows a schematic of the experimental arrangement.

Gas was supplied through a 2 mm thick glass multicapillary array, glued to the top of an aluminum needle having a 2 mm diameter inner bore. This arrangement provided a well-localized high density gas target without dramatically increasing the background pressure inside the vacuum chamber or the pumping speed requirements. The length of the target intersecting the primary ion beam was estimated to be between 3 and 4 mm. A detailed study of this type of gas source has been provided by Steckelmacher et al.[8].

The recoil ions created in the interaction region were allowed to drift through a field free region (3.8 cm long) until they reached the first collimating aperture (3 mm diameter) where they were accelerated through a potential difference V_a. With this configuration the angular acceptance was estimated to be 4°(FWHM). Accelerated recoil ions of charge state q and energy q e V_a, were momentum analyzed by a 90° bending magnet and counted by a channel electron multiplier(CEM). To ensure a detection efficiency independent of the charge state, the entrance cone of the CEM was held at -2500 V.

Special care was taken to keep the recoil ion path free of stray electric and magnetic fields. The interaction region as well as the pre and post analysis regions were shielded with several layers of mu-metal. Ultra high vacuum techniques were used in the design, handling and mounting of the different parts. The base pressure in the chamber was in the upper 10^{-8} Torr range. Single collision conditions were established from linear plots of the total number of recoil ions versus target pressure. The working pressure inside the chamber was 2.5×10^{-5} Torr (true Ne pressure).

Although total cross sections for the production of recoil ions are high, permitting the recoil ions to drift freely to preserve recoil angle information, presented several problems. The solid angle collected by the analyzer is only a small fraction (~1%) of 4π. Furthermore, the slow (~few eV), highly charged ions must drift through a region with gas density higher than the background density for at least a few millimeters. Cross sections for a few degrees elastic scattering between these recoils and the background gas are estimated to be in the order of 10^{-14} cm^2. Together, these factors gave us detected recoil count rates of a few per second (typically less than 20 counts/sec.).

The analyzer viewing angle could be varied from outside the chamber with a reproducibility of 0.1°. The acceleration voltage V_a was fixed at -25 V during the experiment, where the transmission function of the analyzer was observed to reach a plateau. Standard beam normalization techniques were used throughout the experiment. The overall collection efficiency was observed to be extremely sensitive to parameters such as alignment and background pressure.

Results

The observation angle is defined as in Fig.1, increasing from 0° as we move away from the beam direction. For a given charge

state the energy of the recoil ion increases with increasing channel number. Fig.2 presents typical recoil ion spectra for three different recoil angles. In the forward hemisphere (76°-Fig.2(a)) the lower charge state ($q < 4$) appear rather symmetric while for $q=4,5,6$ they display a remarkable skewness towards higher energies. Fig.2(b) corresponds to an observation angle of 88°. We still can see the higher charge states rising suddenly but they extend over a wider energy range. Contributions from overlapping charge states, produce a "hump" type feature. In the backward hemisphere (104°-Fig.2(c)), the spectra show sharp, symmetric and well resolved peaks. The small peak to the right of each principal charge state is due to the Neon isotope with mass 22 (10% abundance). Immediately to the right of Ne^{2+} and Ne^{3+} there are two peaks corresponding to the same mass-to-charge ratios but with higher energies. These peaks are interpreted as being produced by Ne^{3+} and Ne^{4+} ions which undergo exothermic reactions (electron capture) in the drift region and change charge state. The measured energy gain for the ions in both peaks is of the same order as the energy gains reported by Schmeissner et al[9], although our experiments involve collisions at a much lower energy.

A complete angular distribution is shown in Fig.3. In Fig.4 we have plotted the total number of ions collected (Ne^{q+}, $q = 1,\ldots,7$) as a function of the observation angle. The maximum of this distribution lies close to 87°.

Results similar to those presented in Fig.3 were also obtained with 22.5 MeV Cl^{8+} and 33 MeV Cl^{5+} incident on Ne. While we find a change in the relative yield between recoil charge states, all the characteristic features of the angular distributions remain unchanged. This relative change in intensity, even under similar experimental conditions, can be associated with the changes observed in the overall transmission function.

Theory and Discussion

We assume a classical two-body collision, and write the energy and momentum conservation equations in the center of mass system (CMS), including in the energy balance an inelastic term (Q), also known as the reaction energy. Defining M_1, V_1, M_2, V_2 as projectile and target mass and initial velocity respectively and V_3, V_4 as the projectile and target final velocity, we write the energy conservation equation as:

$$Q + E_1 + E_2 = E_3 + E_4 \qquad (1)$$

where the left term contains the initial energies (including the inelasticity Q) for projectile and target, and the right term the corresponding final energies. According to eq.(1) a negative Q value corresponds to an endothermic reaction (projectile and/or target ionization), while a positive Q value yields an exothermic reaction (electron capture by the projectile).

Using the elementary relations derived from momentum conservation in the CMS, and transforming from the CMS to the laboratory system, the final energy of the target recoil(E_{4L}) as well as its ejection angle(θ_{2L}) can be expressed in the laboratory system as:

$$E_{4L} = 2\, M_1\, E_0\, [(1+Q/2E_0) - \cos(\theta_1)\,(1+Q/E_0)^{1/2}]/(M_1+M_2) \qquad (2),$$

$$\theta_{2L} = \tan^{-1}\, \{\sin(\theta_1)/[\cos(\theta_1) - (1+Q/E_0)^{-1/2}]\} \qquad (3)$$

where θ_1 is the projectile scattering angle in the CMS and $E_0 = (M\, V_{1L}^2)/2$ with $M = M_1M_2/(M_1+M_2)$ and V_{1L} the projectile velocity in the laboratory frame.

Equations (2) and (3) show that given a projectile scattering angle θ_1 and reaction energy Q, the recoil energy and ejection angle can easily be calculated. Fig.5 plots E_{4L} versus θ_{2L} for two different Q values. We have used θ_1 as the input variable in both equations and have assumed endothermic reactions ($Q < 0$) which correspond to target and/or projectile ionization.

The relation between recoil ion energy and impact parameter for simple Coulomb scattering is given by

$$E_{4L} = (M_1 \, q_1^2 \, q_2^2)/(M_2 \, b^2 \, E_{1L}) \qquad (4)$$

where q_1, E_{1L} are the projectile effective charge and laboratory energy respectively, q_2 is the recoil effective charge and b is the impact parameter.

We can use eq.(4) to relate the recoil energy E_{4L} and the recoil angle θ_{2L} to the ionization probability P(b) if we assume a functional relation between ionization probability and impact parameter. This is done by using

$$P(b) = b \, e^{-(b/r)} \qquad (5)$$

where P(b) is the probability to remove one electron from the target when the impact parameter for the collision is b. As a crude estimate the decay parameter r can be taken as the expectation value for the radial coordinate of the electronic wave function for the shell under consideration.

In Fig.6 we plot P(b) as a function of recoil ion ejection angle θ_{2L} (Fig.6(a)) and recoil ion energy E_{4L} (Fig.6(b)) for the

case of 22.5 MeV chlorine ions incident on Ne assuming a Q value of -350 eV (equal to the sum of the first five ionization potentials of neon). Effective projectile and target charge q_1 and q_2 used in calculating the curves displayed in Fig.6 were q_1=7 and q_2=5 and radius r=0.6 au. Higher q_1 or q_2 values than the ones used in this calculations give narrower ionization probability distributions, with maxima closer to 90°, than the one shown in Fig.6(a)

The results of Fig.6 can be compared with our experimental findings displayed in Fig.2 and 4. For a given charge state (q>3) the distribution displayed in Fig.2(a) shows similar dependence on energy as the one plotted in Fig.6(b). In addition, the angular dependence shown in Fig.6(a) shows some similarity with the angular distribution displayed in Fig.4. Although in Fig.4 we presented the total number of ions summed over all charge states, similar curves are obtained if yields for individual charge states are plotted.

The mean value for the reaction energy Q can be obtained from eq.(2) and eq(3), using the measured recoil ion energy and ejection angle as the input parameters. As an example, a Ne^{5+} ion with a kinetic energy of 3.5 eV ejected at 76° requires a reaction energy Q ~ -3.5 KeV. Furthermore, the ejection angle from Fig.4, for which the number of ions created is maximum (θ_{2L}~87°), also suggests that predominantly higher Q values are present.

Within this model, recoil ion ejection into the backward hemisphere can only occur for positive values of Q (exothermic reaction). In this case curves displaying recoil energy vs. ejection angle like the one shown in Fig.5 extend across 90° with decreasing recoil energy for larger angles. In order to have an exothermic reaction, the projectile must capture at least one electron from the target. Using the corresponding ionization potentials for the projectile-target combinations employed in the experiment it is not possible to obtain positive Q values except for the lower recoil ion charge states (q=1,2).

Conclusions

We have shown the feasibility of doubly-differential measurements of multiple-ionized low-energy recoil ions. The reaction energy model presented explains only some of the observed effects, indicating that differential information extracted from a more elaborate theory of multiple ionization is needed in order to interpret the results. With small modifications the present experimental setup could be used to perform energy gain spectroscopy of electron capture at incident energies as low as the ones provided by the source itself, extending the energy range for such experiments downward by almost an order of magnitude.

This work was supported in part by the National Science Foundation and by the U.S. DOE under contract No. DE-AC05- 840R21400 with Martin Marietta Energy Systems, Inc.

References

(1) P.Richard, I.L.Morgan, T.Furuta, and D.Burch, Phys.Rev.Lett.23 (1969)1009. J.R.Mowat, I.A.Sellin, D.J.Pegg, R.S.Peterson, M.D.Brown and J.R.Macdonald, Phys.Rev.Lett.30(1973)1289.

(2) C.L.Cocke, Phys.Rev.A20(1979)749.

(3) See Book of Abstracts XIV ICPEAC, Palo Alto,CA 1985.

(4) R.E.Olson, J.Phys.B:Atom.Molec.Phys.12(1979)1843.

(5) M.Horbatsch, Z.Phys.D-Atoms, Mol. and Clusters 1(1986)337.

(6) A.Russek and M.T.Thomas, Phys.Rev.109(1958)2015; 114(1959)1538; J.B.Bulman and A.Russek,ibid.122(1961)506; A.Russek,ibid.132(1963)246. A.Russek and J.Meli, Physica 46(1970)222.

(7) T.J.Gray, C.L.Cocke and E.Justiniano, Phys.Rev. A22(1980)849.

(8) W.Steckelmacher, R.Strong and M.W.Lucas, J.Phys.D:Appl.Phys., 11(1978)1553.

(9) C.Schmeissner,C.L.Cocke,R.Mann and W.Meyerhof, Phys.Rev. A30(1984)1661.

Figures Caption

Fig.1 Schematic of the experimental apparatus.

Fig.2 Spectra of recoil ions obtained for 22.5 MeV Cl^{4+} incident on Ne for three different angles. (a):76°, (b):88°, (c):104° where numbers in parenthesis label different ^{20}Ne charge states. For a given charge state, the energy increases with increasing channel number.

Fig.3 Complete recoil ions angular distribution for 22.5 MeV Cl^{4+} incident on Ne.

Fig.4 Yields of recoil ions as a function of ejection angle summed over all charge states (Ne^{q+}, q=1,...,7). The solid line is to guide the eye through the data.

Fig.5 Plots of recoil ion energy versus ejection angle obtained from eqs.(2) and (3) for (a):Q=-350eV, (b):Q=-1000eV.

Fig.6 Plots of ionization probability vs. (a)ejection angle, (b)recoil energy , see text for details.

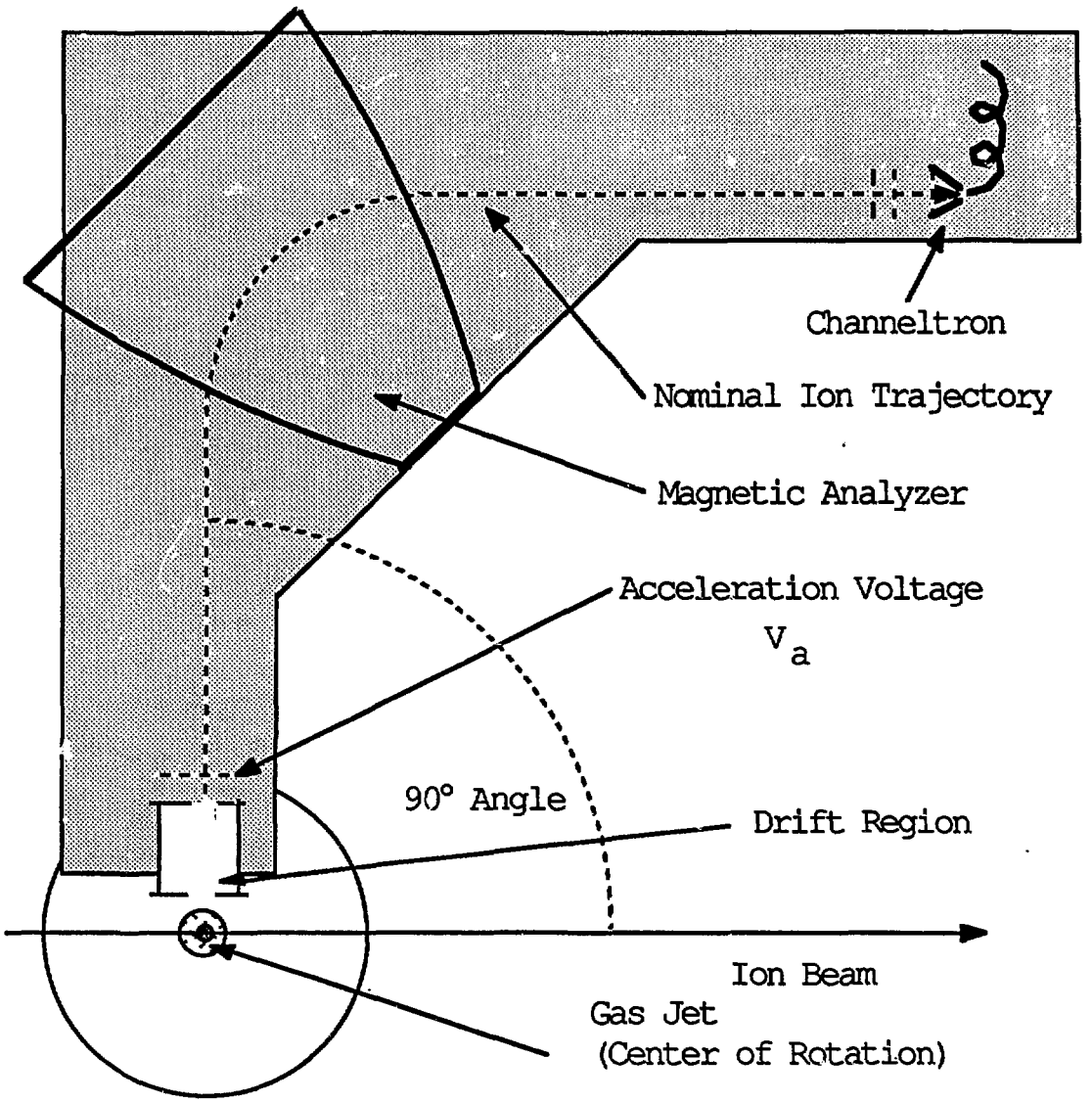
Channeltron
Nominal Ion Trajectory
Magnetic Analyzer
Acceleration Voltage
V_a
90° Angle
Drift Region
Ion Beam
Gas Jet
(Center of Rotation)

Figure 1

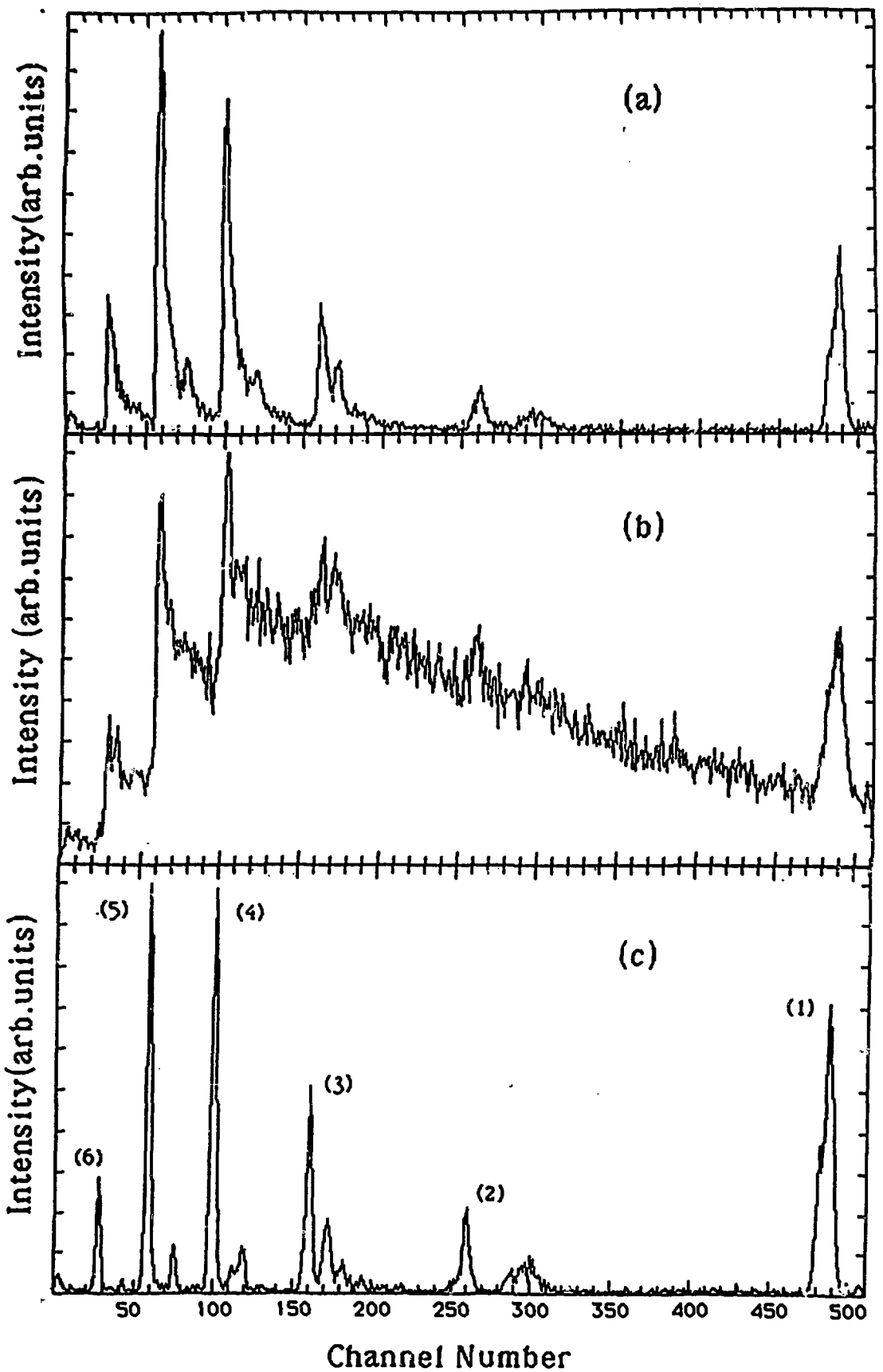
(a)
(b)
(c)
Intensity(arb.units)
Intensity (arb.units)
Intensity(arb.units)
(1)
(2)
(3)
(4)
(5)
(6)
50
100
150
200
250
300
350
400
450
500
Channel Number

Figure 2

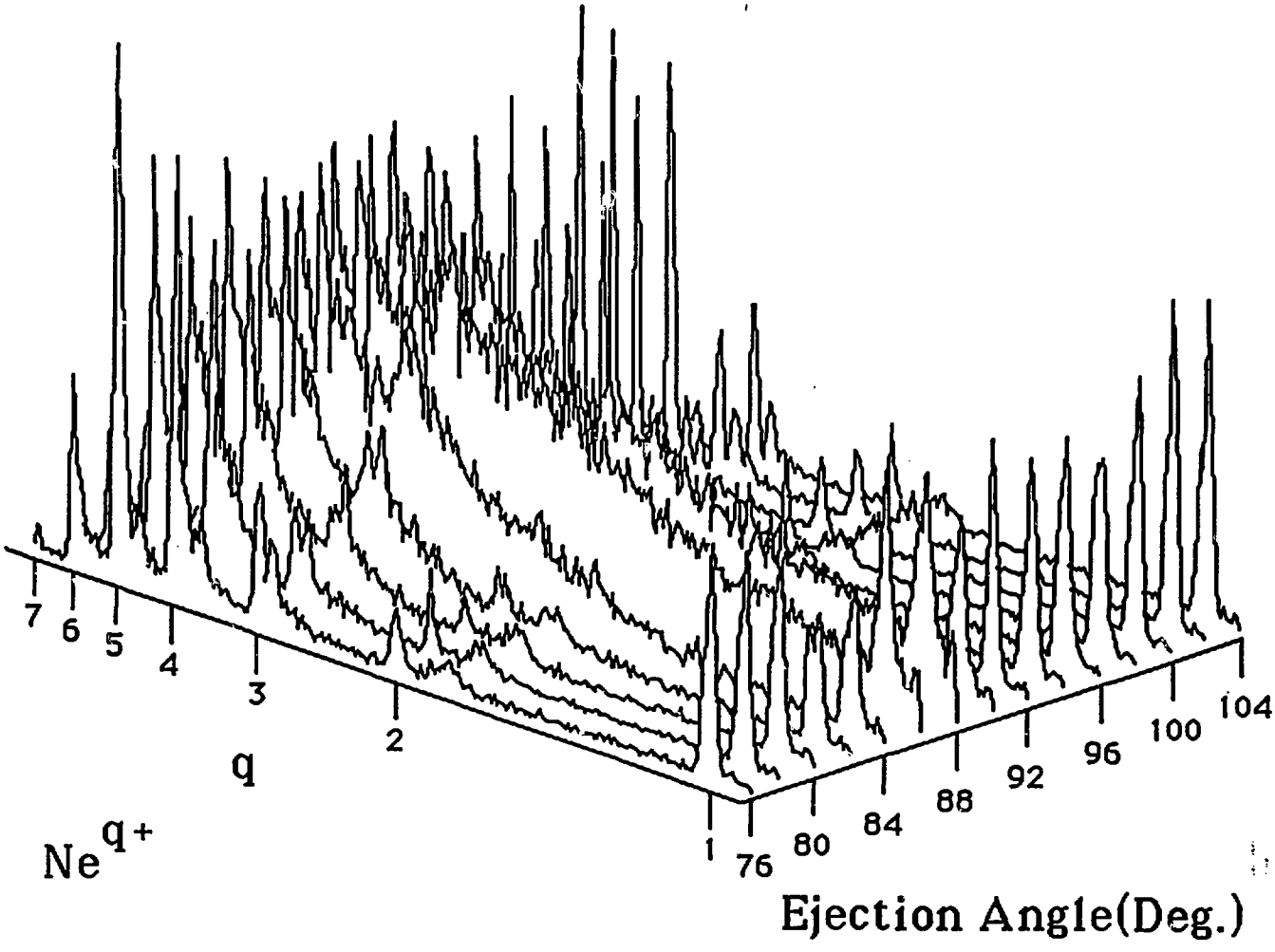

Figure 3

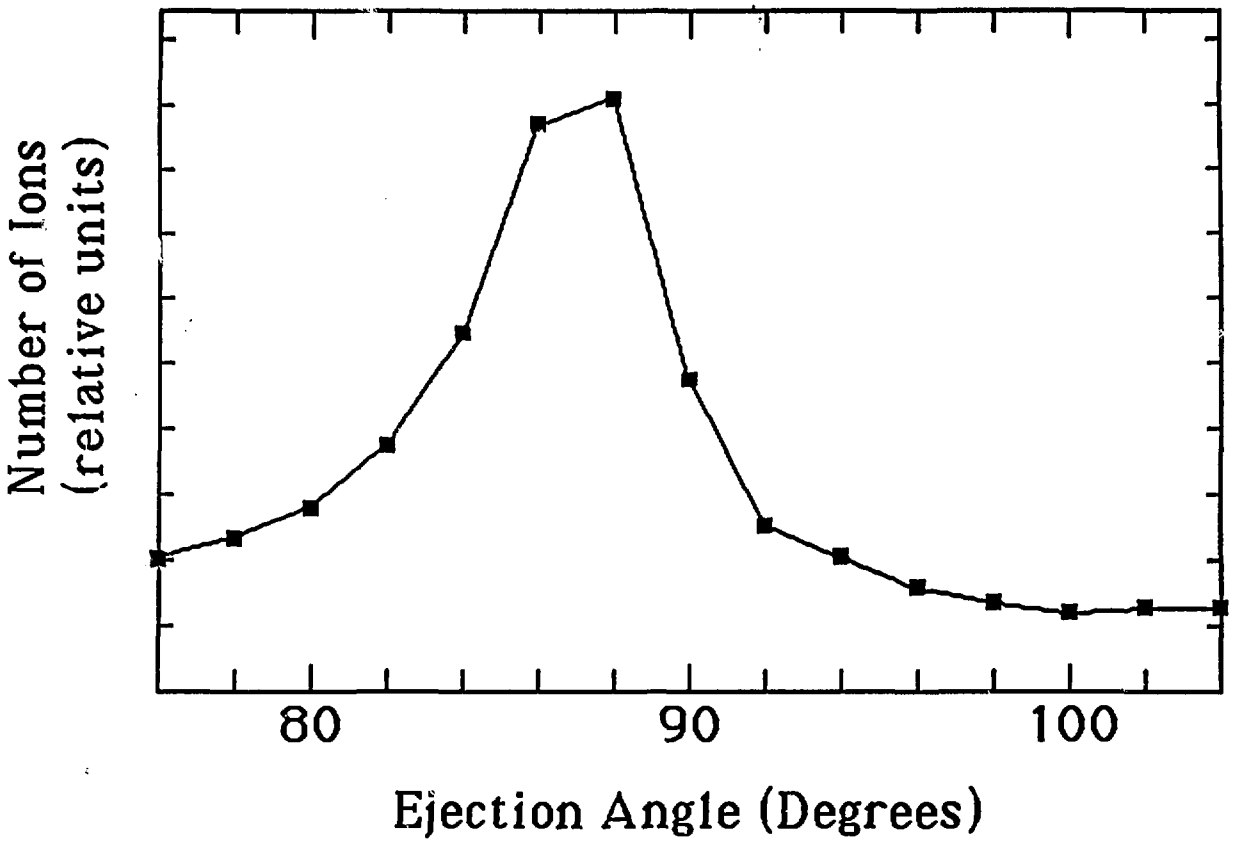
Number of Ions
(relative units)
80
90
100
Ejection Angle (Degrees)

Figure 4

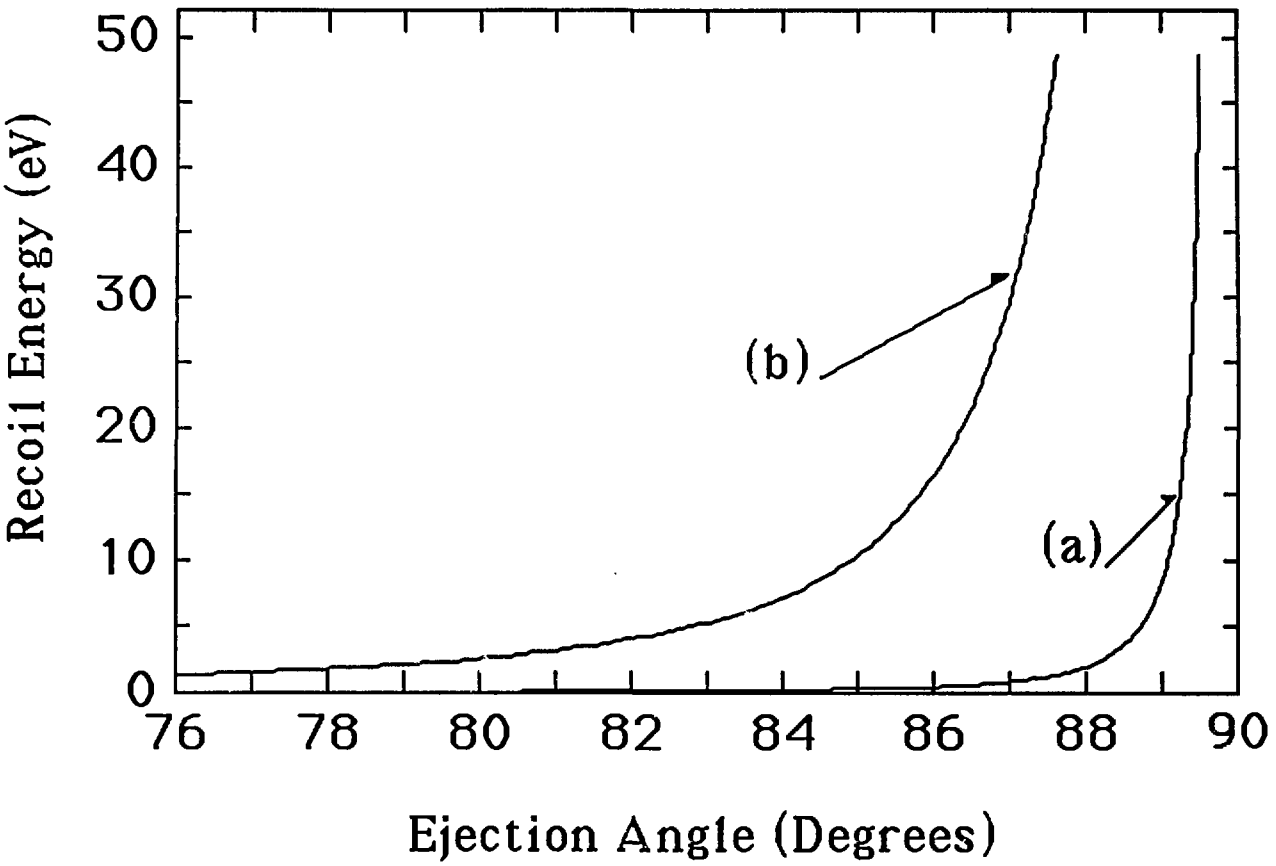
Recoil Energy (eV)
50
40
30
20
10
0
76
78
80
82
84
86
88
90
(b)
(a)
Ejection Angle (Degrees)

Figure 5

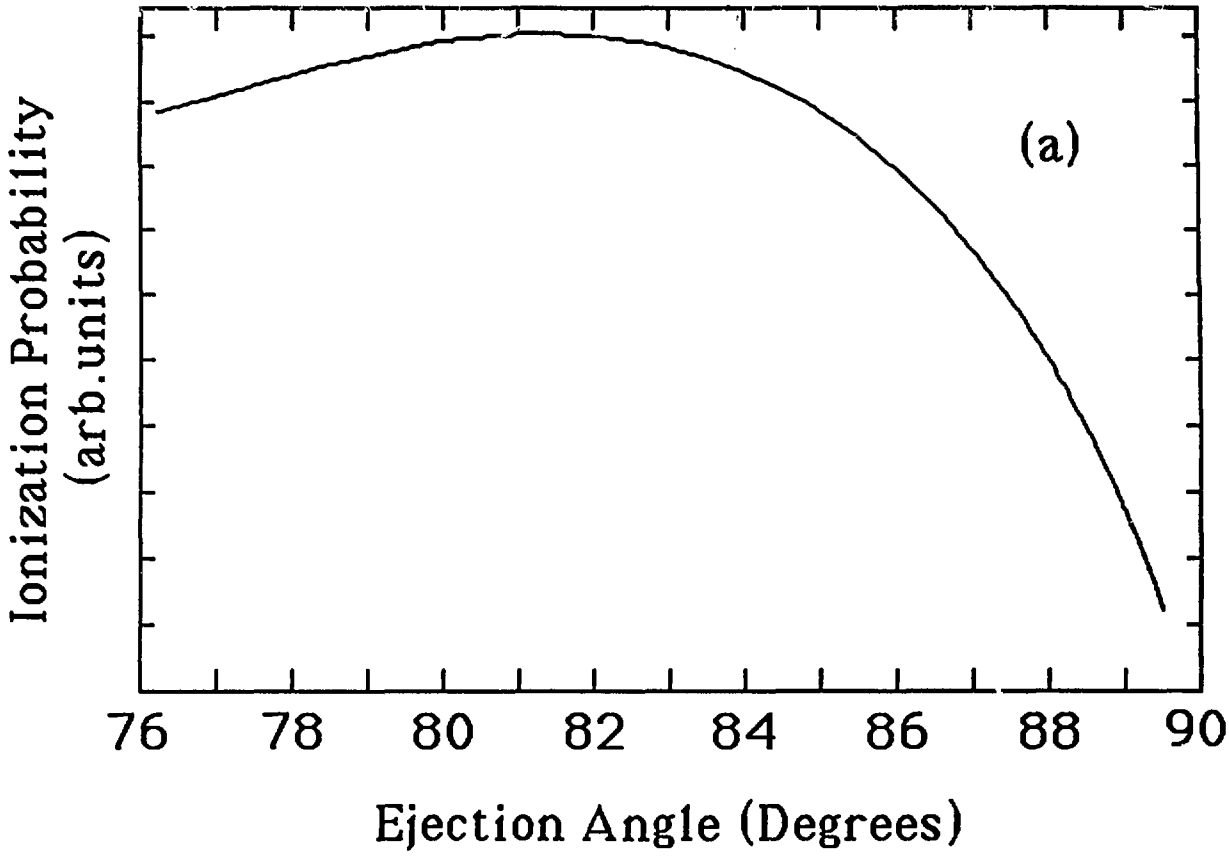
Ionization Probability
(arb.units)
(a)
76
78
80
82
84
86
88
90
Ejection Angle (Degrees)

Figure 6

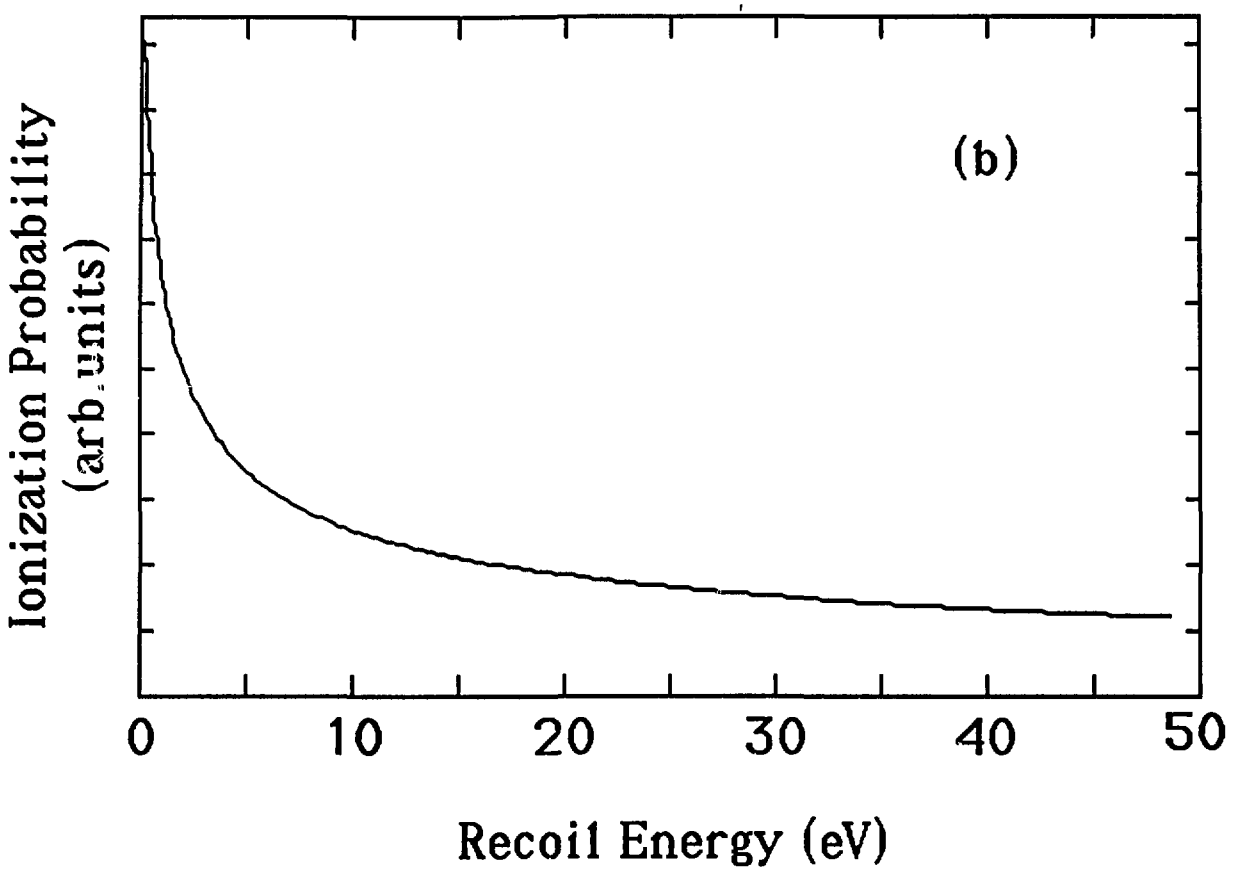
(b)
Ionization Probability
(arb. units)
0
10
20
30
40
50
Recoil Energy (eV)

Figure 6

DISCLAIMER